

Time reversal invariant single-gap superconductivity with upper critical field larger than the Pauli limit in NbIr₂B₂

Debarchan Das ^{1,*} Karolina Górnicka,^{2,3} Zurab Guguchia ¹ Jan Jaroszynski,⁴ Robert J. Cava,⁵ Weiwei Xie,⁶ Hubertus Luetkens,¹ and Tomasz Klimczuk^{2,3,†}

¹Laboratory for Muon Spin Spectroscopy, Paul Scherrer Institute, CH-5232 Villigen PSI, Switzerland

²Faculty of Applied Physics and Mathematics, Gdańsk University of Technology, ulica Narutowicza 11/12, Gdańsk 80233, Poland

³Advanced Materials Centre, Gdańsk University of Technology, ulica Narutowicza 11/12, Gdańsk 80233, Poland

⁴National High Magnetic Field Laboratory, Florida State University, Tallahassee, Florida 32310, USA

⁵Department of Chemistry, Princeton University, Princeton, New Jersey 08540, USA

⁶Department of Chemistry and Chemical Biology, Rutgers University, Piscataway, New Jersey 08854, USA



(Received 26 April 2022; revised 31 August 2022; accepted 1 September 2022; published 14 September 2022)

Recently, compounds with noncentrosymmetric crystal structure have attracted much attention for providing a rich playground in search for unconventional superconductivity. NbIr₂B₂ is a new member to this class of materials harboring superconductivity below $T_c = 7.3(2)$ K and a very high upper critical field that exceeds Pauli limit. Here we report on muon spin rotation (μ SR) experiments probing the temperature and field dependence of effective magnetic penetration depth in this compound. Our transverse-field- μ SR results suggest a fully gapped s -wave superconductivity. Furthermore, the estimated high value of the upper critical field is also supplemented by high-field transport measurements. Remarkably, the ratio $T_c/\lambda^{-2}(0)$ obtained for NbIr₂B₂ (~ 2) is comparable to those of unconventional superconductors. Zero-field μ SR data reveal no significant change in the muon spin relaxation rate above and below T_c , evincing that time-reversal symmetry is preserved in the superconducting state. The presented results will stimulate theoretical investigations to obtain a microscopic understanding of the origin of superconductivity with preserved time-reversal symmetry in this unique noncentrosymmetric system.

DOI: [10.1103/PhysRevB.106.094507](https://doi.org/10.1103/PhysRevB.106.094507)

I. INTRODUCTION

The crystal structure of a noncentrosymmetric superconductor (NCS) lacks a center of inversion favoring an electronic antisymmetric spin orbit coupling (ASOC) to subsist by symmetry [1–5]. For sufficiently large ASOC, one may expect mixing of spin-singlet and spin-triplet Copper pairing channels leading to many exotic superconducting properties, namely, very high upper critical fields higher than the Pauli limit, nodes in the superconducting gaps, appearance of tiny spontaneous fields below the superconducting transition temperature T_c , breaking time-reversal symmetry (TRS) etc. [4,5]. For this reason, NCSs are of significant interest and have become an intensively studied topic in contemporary condensed-matter research.

There are quite a few examples of NCSs in the literature, e.g., CePt₃Si [6], Ce(Rh,Ir)Si₃ [7,8], LaNiC₂ [9], La₇Ir₃ [10], Re_xT_y series ($T = 3d-5d$ early transition metals) [11–14], Mg₁₀Ir₁₉B₁₆ [15], ARh₂B₂ ($A = \text{Nb}$ and Ta) [16–18], etc., [4,5,19–25]. Among these wide range of materials, compounds without any magnetic f electron element are of particular interest because it allows to study the intrinsic pairing mechanisms in NCSs. Thus, the search for new NCSs of this class has become an exigent goal. Very recently, we have

discovered two novel Ir-based NCSs NbIr₂B₂ and TaIr₂B₂ forming a unique low symmetry Cc noncentrosymmetric crystal structure [26]. First-principles calculations and symmetry analysis suggest that these materials are topological Weyl metals in the normal state [27]. Bulk measurements reveal superconducting properties having T_c 's 7.2 and 5.1 K along with considerably high value of the upper critical fields 16.3 and 14.7 T, respectively. Interestingly, theoretical calculations signals a possible multigap scenario for NbIr₂B₂. Therefore, a detailed microscopic experimental study is essential to address this intriguing aspect. Muon spin rotation/relaxation (μ SR) [28–30] is a very sensitive technique to probe the superconducting gaps and the nature of the pairing in superconductors. In the case of a type-II superconductor, the mixed or vortex state creates flux line lattice (FLL) which gives rise to an inhomogeneous spatial distribution of local magnetic fields influencing the muon spin depolarization rate. It is directly related to the magnetic penetration depth λ which is one of the fundamental length scales of a superconductor. The temperature dependence of λ is sensitive to the structure of the superconducting gap. Moreover, zero-field μ SR is a very powerful tool to detect the presence of infinitesimally small magnetic field which is crucial in verifying whether TRS is broken in the superconducting state.

In this paper, we present the results of our detailed μ SR investigation performed on NbIr₂B₂ aiming to unravel the superconducting gap structure and to check whether the TRS is broken or preserved in the superconducting state. In addition,

*debarchanddas.phy@gmail.com

†tomasz.klimczuk@pg.edu.pl

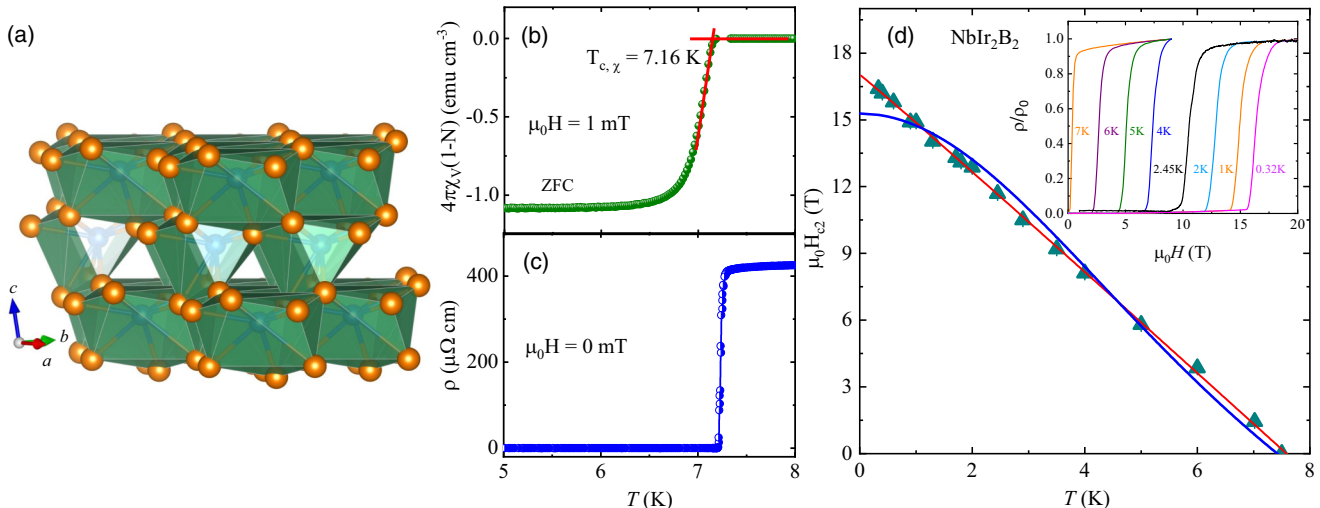


FIG. 1. (a) Crystal structure of NbIr_2B_2 . Orange spheres represent Nb atoms and Ir atoms are shown as blue spheres. For better clarity B-B dimers are not presented in the figure. (b) Temperature dependence of magnetic susceptibility measured in a zero-field-cooled condition under 1-mT applied field. (c) Zero-field electrical resistivity (ρ) as a function of temperature. (d) $\mu_0 H_{c2}(T)$ phase diagram. Red and blue solid lines correspond to the fitting using different models as discussed in the text. The inset: field dependence of normalized resistivity (ρ/ρ_0) measured at different temperatures. Only few selected temperatures are shown for clarity.

we also report electrical transport measurements under high magnetic fields (up to 20 T) down to 300 mK to extract more reliable value of upper critical field. Our results evince fully gap s -wave pairing with preserved time-reversal symmetry in NbIr_2B_2 possessing a very high value of an upper critical field.

II. EXPERIMENTAL DETAILS

A polycrystalline sample of NbIr_2B_2 was prepared by a solid-state reaction method of the constituent elements. The detailed procedure of sample preparation can be found in Ref. [26]. Phase purity of the polycrystalline sample was checked by powder x-ray diffraction (XRD) using $\text{Cu } K\alpha$ radiation and other metallographic experiments, such as scanning electron microscopy and energy-dispersive x-ray spectroscopy. The details of Rietveld analysis together with crystallographic data can be found in Ref. [26]. A NbIr_2B_2 sample for magnetotransport measurements was prepared in a bar form with four 50- μm diameter platinum wire leads spark welded to the sample surface. Transverse-field (TF) and zero-field (ZF) μSR experiments were carried out at the Paul Scherrer Institute (Villigen, Switzerland). The measurements down to 1.5 K were performed at the $\pi\text{M3.2}$ beamline using a GPS spectrometer, and measurements down to 270 mK were conducted at the πE1 beamline on the DOLLY spectrometer. The powdered sample was pressed into a 7-mm pellet which was then mounted on a Cu holder using GE varnish. This holder assembly was then mounted in the respective spectrometer cryostats. Both spectrometers are equipped with a standard veto setup [31] providing a low-background μSR signal. All the TF experiments were performed after field-cooled cooling the sample. The μSR time spectra were analyzed using the MUSRFIT software package [32].

III. RESULTS

A. Crystal structure, sample characterization, and high magnetic-field measurements

Figure 1(a) shows the crystal structure of NbIr_2B_2 . The same type of polyhedrons, oriented in different directions, are formed by Nb atoms with an Ir atom inside. For clarity B-B dimers, which are located in voids of the polyhedrons, are not presented in the figure. The superconductivity of the samples was confirmed by magnetic susceptibility and electrical resistivity measurements. Figure 1(b) shows the temperature dependence of magnetic susceptibility (measured in zero-field-cooled condition in an applied field of 1 mT) which manifests a diamagnetic signal below $T_{c,x} = 7.16$ K concurrent with the offset of zero-resistivity [Fig 1(c)]. These results highlight the good quality of the sample with superconducting properties matching well with our previous report [26].

Figure 1(d) represents the upper critical field-temperature [$\mu_0 H_{c2}(T)$] phase diagram determined from field-dependent electrical transport measurements performed at National High Magnetic Field Laboratory. The data points were obtained from ρ vs $\mu_0 H$ measurements carried out at constant temperatures. Selected curves are shown in the inset of Fig. 1(d) (presented as normalized resistivity). The critical field at each temperature was estimated as a midpoint of the transition. It is worth noting that the superconducting transition only slightly broadens under the highest applied magnetic field. It is quite evident from the linear temperature dependence of the upper critical field that $\mu_0 H_{c2}(T)$ cannot be modeled using the Werthamer-Helfand-Hohenberg model [33] which accounts for Pauli limiting and spin-orbit scattering effects. We used the following model to describe the temperature dependence of upper critical field $\mu_0 H_{c2}(T) = \mu_0 H_{c2}(0)[1 - (T/T_c)^n]$ yielding $n = 1.02(2)$ and $\mu_0 H_{c2}(0) = 17.0(1)$ T. Notably, thus, the obtained value of $\mu_0 H_{c2}(0)$ is considerably higher than

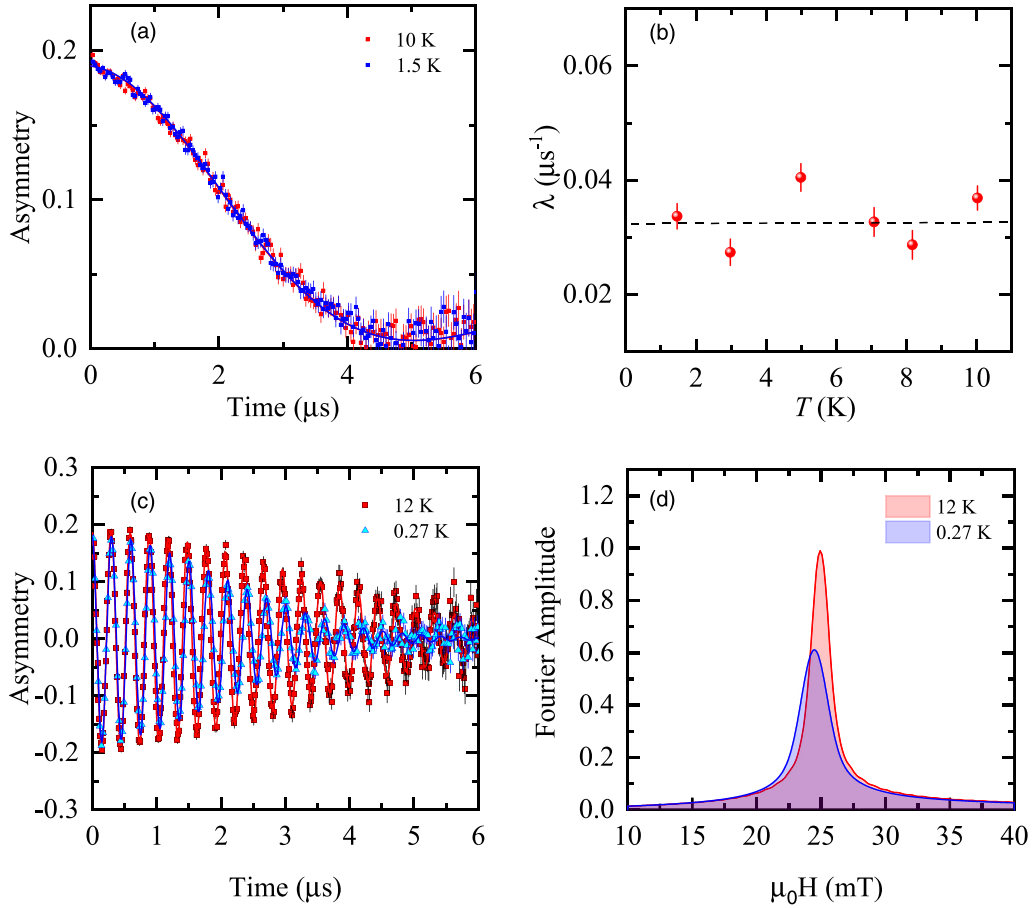


FIG. 2. (a) ZF μ SR asymmetry spectra recorded at 1.5 and 10 K for NbIr_2B_2 . (b) Temperature dependence of the electronic relaxation rate measured in zero magnetic field. (c) TF μ SR time spectra obtained above and below T_c for NbIr_2B_2 in an applied field of 25 mT (after field cooling the sample from above T_c). (d) Fourier spectra at 0.27 K (blue) and 12 K (red) obtained by fast Fourier transformation of the μ SR time spectra from panel (c).

the Pauli-limiting field [13.3(1) (T)] signaling non-BCS-type superconductivity in NbIr_2B_2 . To model the data, we also tested the Ginzburg-Landau expression [34],

$$\mu_0 H_{c2}(T) = \mu_0 H_{c2}(0) \frac{(1 - t^2)}{(1 + t^2)}, \quad (1)$$

where $t = T/T_c$ and T_c is the transition temperature at zero magnetic field. As seen from the fitting (blue solid line), this model does not work in the present case.

B. ZF- μ SR measurements

In NCSs, due to the admixture of spin-singlet and spin-triplet superconducting channels, small magnetic moments associated with the formation of spin-triplet electron pairs might appear in the superconducting state. Thus, NCSs are prime candidates to search for novel superconductors showing TRS breaking. To explore this tempting issue in this novel NCS NbIr_2B_2 , we first performed ZF- μ SR experiments above and below T_c to detect any possible spontaneous magnetic fields which lead to broken TRS. Figure 2(a) shows the ZF- μ SR asymmetry spectra for temperatures above and below T_c . We do not observe any noticeable difference in the spectra

suggesting absence of any spontaneous field in the superconducting state. The ZF- μ SR asymmetry spectra can be well described by a damped Gaussian Kubo-Toyabe depolarization function [35] $A_{ZF}(t) = A_0 G_{KT} \exp(-\Lambda t)$ where A_0 is the initial asymmetry, G_{KT} is the Gaussian Kubo-Toyabe (KT) function [35] which accounts for an isotropic Gaussian distribution of randomly oriented static (or quasistatic) local fields at the muon sites, and Λ is the electronic relaxation rate. Figure 2(b) represents the temperature dependence of Λ which shows no considerable enhancement across T_c . The maximum possible spontaneous flux density due to superconductivity can be estimated using $(\Lambda|_{1.5\text{K}} - \Lambda|_{10\text{K}})/(2\pi\gamma_\mu) = 0.43 \mu\text{T}$ which is several times smaller than that seen for well-known TRS breaking superconductors [9,10,13,36]. We note that even though the field resolution of the instrument is finite, it is sufficient to detect an internal field of the magnitude found in other superconductors where time-reversal symmetry breaking was observed. Therefore, it can be concluded that the time-reversal symmetry is preserved in the superconducting state of NbIr_2B_2 . Electronic structure calculation presented in our earlier report [26] manifests that in spin-split bands $E(k) = E(-k)$ degeneracy is kept whereas the spin direction is flipped without giving rise to any net moment as k

is changed to $-k$. Therefore, the absence of time-reversal symmetry breaking in the superconducting state is consistent with the electronic structure calculation.

C. TF- μ SR measurements

Figure 2(c) represents TF- μ SR spectra for NbIr₂B₂ measured in an applied magnetic field of 25 mT at temperatures above (12-K) and below (0.27-K) T_c . Above T_c , we observed a small relaxation in TF- μ SR spectra due to the presence of random local fields associated with the nuclear magnetic moments. However, in the superconducting state, the formation of FLL causes an inhomogeneous distribution of magnetic field which increases the relaxation rate of the μ SR signal. Assuming a Gaussian field distribution, we analyzed the observed TF- μ SR asymmetry spectra using the following functional form:

$$A_{TF}(t) = A_0 \exp(\sigma^2 t^2 / 2) \cos(\gamma_\mu B_{\text{int}} t + \varphi), \quad (2)$$

where A_0 refers to the initial asymmetry, $\gamma_\mu / (2\pi) \simeq 135.5$ MHz/T is the muon gyromagnetic ratio, and φ is the initial phase of the muon-spin ensemble, B_{int} corresponds to the internal magnetic field at the muon site, respectively, and σ is the total relaxation rate. Here, σ is related to the superconducting relaxation rate σ_{SC} , following the relation $\sigma = \sqrt{\sigma_{\text{nm}}^2 + \sigma_{\text{SC}}^2}$ where σ_{nm} is the nuclear contributions which is assumed to be temperature independent. For estimating σ_{SC} , we considered the value of σ_{nm} obtained above T_c where only nuclear magnetic moments contribute to the muon depolarization rate σ and kept it fixed. The fits to the observed spectra with Eq. (2) are shown in solid lines in Fig. 2(c). Figure 2(d) depicts the Fourier transform amplitudes of the TF- μ SR asymmetry spectra recorded at 12 and 0.27 K [Fig. 2(c)]. We observed a sharp peak in the Fourier amplitude around 25 mT (external applied field) at 12 K confirming homogeneous field distribution throughout the sample. Notably, a fairly broad signal with a peak position slightly shifted to lower value (diamagnetic shift) was seen at 0.27 K evincing the fact that the sample is indeed in the superconducting mixed state where the formation of the FLL causes such broadening of the line shape.

In Fig. 3(a), we have presented σ_{SC} as a function of temperature for NbIr₂B₂ measured at an applied field of 25 mT. Below T_c , the relaxation rate σ_{SC} increases from zero due to inhomogeneous field distribution caused by the formation of FLL and saturates at low temperatures. In the following section, we show that the observed temperature dependence of σ_{SC} , which reflects the topology of the superconducting gap, is consistent with the presence of the single gap on the Fermi surface of NbIr₂B₂. Figure 3(b) shows the temperature dependence of the relative change in the internal field normalized to the external applied field $\Delta B/B_{\text{ext}} (= \frac{B_{\text{int}} - B_{\text{ext}}}{B_{\text{ext}}})$. As seen from the figure, internal field values in the superconducting state (i.e., $T < T_c$) are lower than the applied field because of the diamagnetic shift, expected for type-II superconductors.

Considering a perfect triangular vortex lattice, the muon spin depolarization rate $\sigma_{\text{SC}}(T)$ is directly related to the

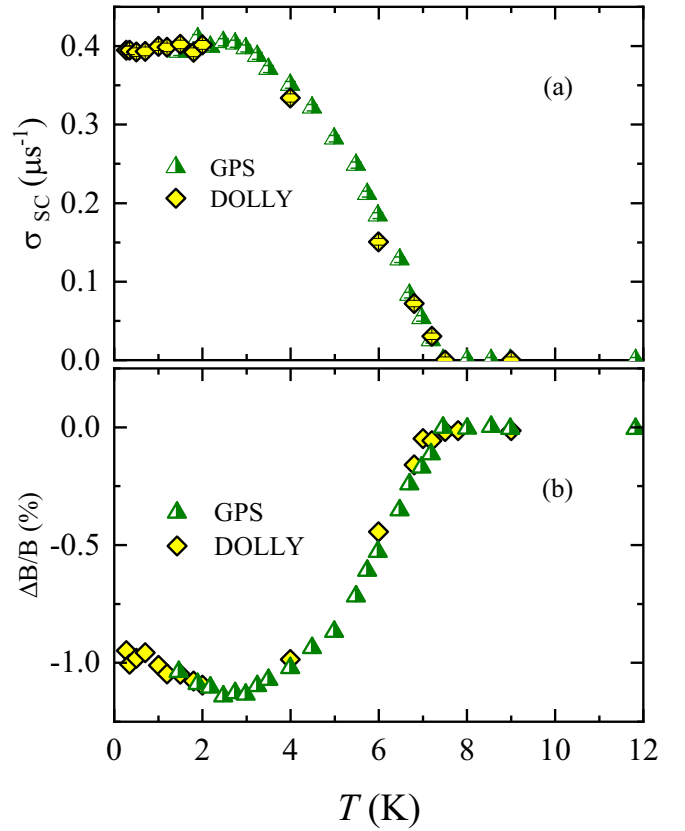


FIG. 3. (a) Temperature evolution of the superconducting muon spin-depolarization rate σ_{sc} of NbIr₂B₂ measured in an applied magnetic field of 25 mT. (b) Temperature dependence of the relative change in the internal field normalized to the external applied field $\Delta B/B_{\text{ext}} (= \frac{B_{\text{int}} - B_{\text{ext}}}{B_{\text{ext}}})$.

London magnetic penetration depth $\lambda(T)$ by [37,38]

$$\frac{\sigma_{\text{sc}}^2(T)}{\gamma_\mu^2} = 0.00371 \frac{\Phi_0^2}{\lambda^4(T)}. \quad (3)$$

Here, $\Phi_0 = 2.068 \times 10^{-15}$ Wb is the magnetic flux quantum. We note that Eq. (3) is only valid when the separation between the vortices is smaller than λ which is presumed to be field independent in this model [37]. To gain insight about the superconducting gap structure of NbIr₂B₂ and estimate various parameters defining the superconducting state of this system, we analyzed the temperature dependence of the magnetic penetration depth $\lambda(T)$.

Within the London approximation ($\lambda \gg \xi$), $\lambda(T)$ can be described by the following expression [32,34,39]:

$$\frac{\lambda^{-2}(T, \Delta_{0,i})}{\lambda^{-2}(0, \Delta_{0,i})} = 1 + \frac{1}{\pi} \int_0^{2\pi} \int_{\Delta(T,\varphi)}^{\infty} \left(\frac{\partial f}{\partial E} \right) \frac{E dE}{\sqrt{E^2 - \Delta_i(T, \varphi)^2}}, \quad (4)$$

where $f = [1 + \exp(E/k_B T)]^{-1}$ is the Fermi function, φ is the azimuthal angle along the Fermi surface, and $\Delta_{0,i}(T) = \Delta_{0,i} \Gamma(T/T_c) g(\varphi)$. $\Delta_{0,i}$ is the maximum gap value at $T = 0$ K. The temperature dependence of the gap is described by the expression $\Gamma(T/T_c) = \tanh\{1.82[1.018(T_c/T - 1)]^{0.51}\}$ [40]. The angular dependence $g(\varphi)$ takes the value of 1 for the s -wave gap whereas for a nodal d -wave gap it is $|\cos(2\varphi)|$.

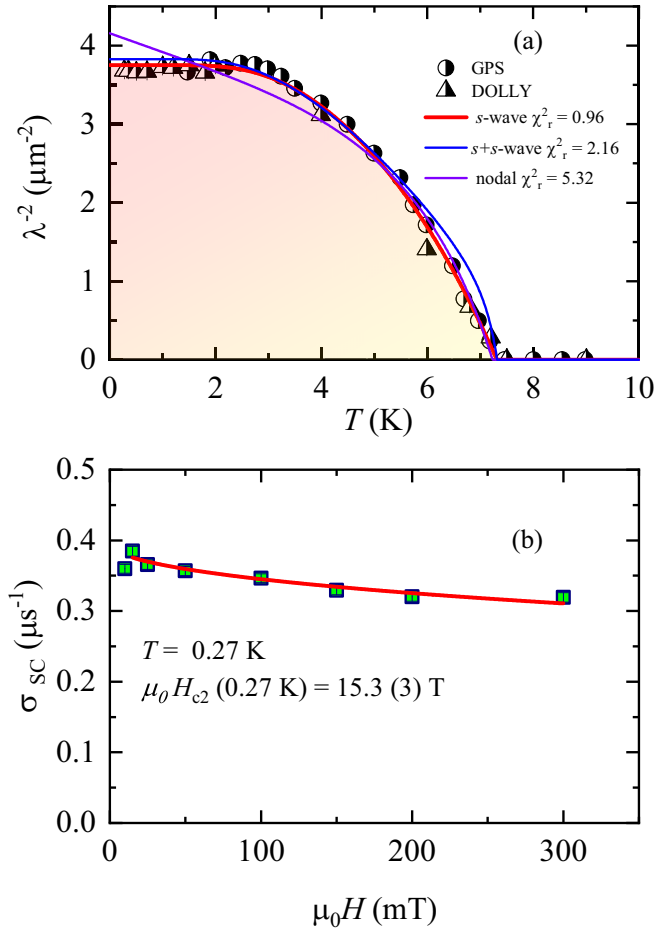


FIG. 4. (a) Temperature dependence of λ^{-2} for NbIr_2B_2 , measured in an applied field $\mu_0 H = 25$ mT. The solid lines correspond to different theoretical models as discussed in the text. (b) Field dependence of the superconducting muon spin depolarization rate at 0.27 K fitted with an isotropic single s -wave gap model (solid red line).

In the present case, as seen from Fig. 4(a), the experimentally obtained $\lambda^{-2}(T)$ is best described by a momentum-independent single s -wave model with a gap value of $\Delta_0 = 1.32(2)$ meV and $T_c = 7.3(2)$ K. Thus, obtained T_c is in good agreement with that estimated from other measurements [see Fig. 1(b)]. In our previous report [26], the specific-heat data were fitted using two models: single-gap s wave and two-gap $s + s$ wave. Interestingly, the gap value determined from μSR studies matches very well with that obtained previously using a single gap [1.35(6)-meV] s -wave model [26]. Our attempt to model $\lambda^{-2}(T)$ using two gaps was unsuccessful as the relative weight of the gaps was reaching a value close to 0, implying a single gap is more appropriate. Furthermore, we also tried to fit the data fixing the gap values to those obtained in Ref. [26] [blue solid line in Fig. 4(a)]. This also failed to model the experimentally observed temperature dependence of $\lambda^{-2}(T)$. We note that even though the $(s + s)$ -wave picture describes the heat-capacity data slightly better [26], the question whether NbIr_2B_2 is a single-gap s -wave or the two-gap $(s + s)$ -wave superconductor remained speculative.

Therefore, from the μSR experiments we confirm the presence of single superconducting gap.

To further corroborate a fully gapped state, we performed the field dependence of the TF- μSR experiments. The TF-relaxation rate $\sigma_{\text{sc}}(B)$ measured at 0.27 K is shown in Fig. 4(b). During measurement, each point was obtained by field cooling the sample from 12 K (above T_c) to 0.27 K. σ_{sc} first increases with increasing magnetic field until reaching a maximum at 15 mT followed by a continuous decrease up to the highest field (300 mT) investigated. Such field dependence resembles with the form expected for a single-gap s -wave superconductor with an ideal triangular vortex lattice. Furthermore, the observed $\sigma_{\text{sc}}(B)$ curve at fields above the maximum, can be analyzed using the Brandt formula (for an s -wave superconductor) [38],

$$\sigma_{\text{sc}}[\mu\text{s}^{-1}] = 4.83 \times 10^4 \left(1 - \frac{H}{H_{c2}}\right) \times \left[1 + 1.21 \left(1 - \sqrt{\frac{H}{H_{c2}}}\right)^3\right] \lambda^{-2} [\text{nm}^{-2}]. \quad (5)$$

which provides an estimate of upper critical field at 0.27-K $\mu_0 H_{c2}(0.27 \text{ K}) = 15.8(3)$ T which is in good agreement with the value obtained from the electrical resistivity measurements (see above).

IV. DISCUSSION

The upper critical field-temperature phase diagram manifests a linear relationship [Fig. 1(d)]. Such behavior is quite rare and strongly suggests unconventional superconductivity in NbIr_2B_2 . It is worth noting that a nearly linear $\mu_0 H_{c2}(T)$ behavior was observed previously in two-band superconductors $\text{Lu}_2\text{Fe}_3\text{Si}_5$ [41] and $\text{Ba}(\text{Fe}_{1-x}\text{Co}_x)_2\text{As}_2$ [42]. However, Kogan and Prozorov showed that $H_{c2}(T)$ linearity might be caused by competing effects of the equatorial nodes and of the Fermi-surface anisotropy [43].

Considering the $\lambda^{-2}(T)$ dependence observed for NbIr_2B_2 , it is important to note that the $(p_x + ip_y)$ pairing symmetry is also characterized by the full gap and would also give saturated behavior of $\lambda^{-2}(T)$ at low temperatures. But, the possibility of $p_x + ip_y$ pairing can be unequivocally excluded by the absence of the TRS-breaking state. Furthermore, to outwit any possibility of having nodes (see the Supplemental Material of Ref. [26]) in the superconducting gap structure, we also tested nodal gap symmetry [see Fig 4(a)], which was found to be inconsistent with the data. Therefore, we ascertain a nodeless or fully gapped state as the most plausible superconducting pairing state in NbIr_2B_2 . This conclusion is also supported by the field dependence of the depolarization rate.

The ratio of the superconducting gap to T_c was estimated to be $(2\Delta_0/k_B T_c) \sim 4.2$ which is consistent with the strong-coupling limit BCS superconductors [44]. Interestingly, for the Bose-Einstein condensation- (BEC-) like picture, a similar ratio can also be expected. Thus, just from the ratio $2\Delta_0/k_B T_c$, we cannot effectively distinguish between BCS or BEC condensations [45]. In this regard, the $T_c/\lambda^{-2}(0)$ ratio is a quite crucial parameter to address this conjecture. Within

the picture of BEC to BCS crossover [46,47], systems exhibiting small $T_c/\lambda^{-2}(0)$ are considered to be on the BCS-like side, whereas the large value of $T_c/\lambda^{-2}(0) \sim 120$ and the linear relationship between T_c and $\lambda^{-2}(0)$ is expected only on the BEC-like side and is considered a hallmark feature of unconventional superconductivity [44,48–50]. For NbIr₂B₂, we obtained the ratio T_c [K]/ $\lambda^{-2}(0)$ [μm^{-2}] ~ 2 which is intermediate between the values observed for electron-doped [$T_c/\lambda^{-2}(0) \sim 1$] and hole-doped [$T_c/\lambda^{-2}(0) \sim 4$] cuprates [46,47,51]. This result yields strong evidence for an unconventional pairing mechanism in NbIr₂B₂ which also exhibits linear temperature dependency of the upper critical field.

In unconventional superconductors, one of the important parameters defining superconductivity is the superconducting carrier density n_s . Within the London theory [28], the penetration depth is directly related to microscopic quantities, such as the effective mass, m^* , and n_s via the relation $\lambda^2(0) = (m^*/\mu_0 n_s e^2)$. Here, m^* can be estimated from the relation $m^* = (1 + \lambda_{e\text{-ph}})m_e$, where $\lambda_{e\text{-ph}}$ is the electron-phonon coupling constant which was previously found out to be 0.74 from heat capacity [26], and m_e is the electron rest mass. From $\lambda^{-2}(T)$ dependence, we determined $\lambda(0) = 516$ (3) nm. Thus, for NbIr₂B₂, we estimated $n_s = 1.88 \times 10^{26} \text{ m}^{-3}$. This value is comparable to that observed in other unconventional superconductors, namely, ZrRuAs ($n_s = 2.1 \times 10^{26} \text{ m}^{-3}$) [21], Nb_{0.25}Bi₂Se₃ ($n_s = 0.25 \times 10^{26} \text{ m}^{-3}$) [52], K₂Cr₃As₃ ($n_s = 2.7 \times 10^{27} \text{ m}^{-3}$) [53], etc. Thus, the relatively high value of T_c and low value of n_s in NbIr₂B₂ are also suggestive of unconventional superconductivity in this compound. The previous band-structure calculation [26] shows existence of two Fermi-surface sheets in NbIr₂B₂. Therefore, Hall conductivity measurements are called for on this compound. This will be decisive to address the question whether the single-gap superconductivity in NbIr₂B₂ as seen through the microscopic experimental probe, such as μ SR, originates from the

superconducting gap occurring only on an electron or holelike Fermi surface.

V. CONCLUSION

In conclusion, we provide a detailed microscopic understanding of the superconducting gap structure of novel noncentrosymmetric superconductor NbIr₂B₂. The temperature as well as the field dependence of λ^{-2} was investigated by means of μ SR experiments which allowed us to determine the zero-temperature magnetic penetration depth $\lambda(0)$. Interestingly, the $T_c/\lambda^{-2}(0)$ ratio is comparable to those of high-temperature unconventional superconductors, signaling the unconventional nature of superconductivity in this compound. The linear temperature dependence of upper critical field also supports this idea. Furthermore, μ SR, which is an extremely sensitive magnetic probe, reveals the absence of any spontaneous magnetic fields that would be expected for a TRS-breaking state in the bulk of NbIr₂B₂. Therefore, our results classify NbIr₂B₂ as an unconventional time-reversal invariant and single-gap superconductor.

ACKNOWLEDGMENTS

The muon spectroscopy studies were performed at the Swiss Muon Source (S μ S) Paul Scherrer Institute, Villigen, Switzerland. D.D. and Z.G. thank C. Baines for the technical assistance during DOLLY experiments. A portion of this work was performed at the National High Magnetic Field Laboratory, which is supported by National Science Foundation Cooperative Agreement No. DMR-1644779 and the State of Florida. The research performed at Gdańsk Technology was supported by the National Science Centre (Poland) Grant No. (UMO-2018/30/M/ST5/00773).

-
- [1] E. Bauer and M. Sigrist, *Non-Centrosymmetric Superconductors* (Springer, Berlin, 2012)
- [2] M. Smidman, M. B. Salamon, H. Q. Yuan, and D. F. Agterberg, *Rep. Prog. Phys.* **80**, 036501 (2017).
- [3] S. Yip, *Annu. Rev. Condens. Matter Phys.* **5**, 15 (2014).
- [4] S. K. Ghosh, M. Smidman, T. Shang, J. F. Annett, A. D. Hillier, J. Quintanilla, and H. Yuan, *J. Phys.: Condens. Matter* **33**, 033001 (2021).
- [5] T. Shang and T. Shiroka, *Front. Phys.* **9**, 651163 (2021).
- [6] E. Bauer, G. Hilscher, H. Michor, C. Paul, E. W. Scheidt, A. Griбанov, Y. Seropegin, H. Noël, M. Sigrist, and P. Rogl, *Phys. Rev. Lett.* **92**, 027003 (2004).
- [7] N. Kimura, K. Ito, K. Saitoh, Y. Umeda, H. Aoki, and T. Terashima, *Phys. Rev. Lett.* **95**, 247004 (2005)
- [8] I. Sugitani, Y. Okuda, H. Shishido, T. Yamada, A. Thamizhavel, E. Yamamoto, T. D. Matsuda, Y. Haga, T. Takeuchi, R. Settai, and Y. Onuki, *J. Phys. Soc. Jpn.* **75**, 043703 (2006).
- [9] A. D. Hillier, J. Quintanilla, and R. Cywinski, *Phys. Rev. Lett.* **102**, 117007 (2009)
- [10] J. A. T. Barker, D. Singh, A. Thamizhavel, A. D. Hillier, M. R. Lees, G. Balakrishnan, D. McK. Paul, and R. P. Singh, *Phys. Rev. Lett.* **115**, 267001 (2015)
- [11] R. P. Singh, A. D. Hillier, B. Mazidian, J. Quintanilla, J. F. Annett, D. McK. Paul, G. Balakrishnan, and M. R. Lees, *Phys. Rev. Lett.* **112**, 107002 (2014).
- [12] D. Singh, J. A. T. Barker, A. Thamizhavel, D. McK. Paul, A. D. Hillier, and R. P. Singh, *Phys. Rev. B* **96**, 180501(R) (2017).
- [13] T. Shang, M. Smidman, S. K. Ghosh, C. Baines, L. J. Chang, D. J. Gawryluk, J. A. T. Barker, R. P. Singh, D. McK. Paul, G. Balakrishnan, E. Pomjakushina, M. Shi, M. Medarde, A. D. Hillier, H. Q. Yuan, J. Quintanilla, J. Mesot, and T. Shiroka, *Phys. Rev. Lett.* **121**, 257002 (2018)
- [14] T. Shang, C. Baines, L.-J. Chang, D. J. Gawryluk, E. Pomjakushina, M. Shi, M. Medarde, and T. Shiroka, *npj Quantum Mater.* **5**, 76 (2020).
- [15] A. A. Aczel, T. J. Williams, T. Goko, J. P. Carlo, W. Yu, Y. J. Uemura, T. Klimczuk, J. D. Thompson, R. J. Cava, and G. M. Luke, *Phys. Rev. B* **82**, 024520 (2010)

- [16] E. M. Carnicom, W. Xie, T. Klimczuk, J. Lin, K. Gornicka, Z. Sobczak, N. Phuan Ong, and R. J. Cava, *Sci. Adv.* **4**, eaar7969 (2018).
- [17] D. A. Mayoh, A. D. Hillier, K. Gotze, D. McK. Paul, G. Balakrishnan, and M. R. Lees, *Phys. Rev. B* **98**, 014502 (2018).
- [18] D. A. Mayoh, M. J. Pearce, K. Gotze, A. D. Hillier, G. Balakrishnan, and M. R. Lees, *J. Phys.: Condens. Matter* **31**, 465601 (2019).
- [19] D. Das, R. Gupta, A. Bhattacharyya, P. K. Biswas, D. T. Adroja, and Z. Hossain, *Phys. Rev. B* **97**, 184509 (2018).
- [20] R. Khasanov, R. Gupta, D. Das, A. Amon, A. Leithe-Jasper, and E. Svanidze, *Phys. Rev. Res.* **2**, 023142 (2020).
- [21] D. Das, D. T. Adroja, M. R. Lees, R. W. Taylor, Z. S. Bishnoi, V. K. Anand, A. Bhattacharyya, Z. Guguchia, C. Baines, H. Luetkens, G. B. G. Stenning, Lei Duan, X. Wang, and C. Jin, *Phys. Rev. B* **103**, 144516 (2021).
- [22] T. Shang, W. Xie, D. J. Gawryluk, R. Khasanov, J. Z. Zhao, M. Medarde, M. Shi, H. Q. Yuan, E. Pomjakushina, and T. Shiroka, *New J. Phys.* **22**, 093016 (2020).
- [23] K. P. Sajilesh, K. Motla, P. K. Meena, A. Kataria, C. Patra, K. Somesh, A. D. Hillier, and R. P. Singh, *Phys. Rev. B* **105**, 094523 (2022).
- [24] Sajilesh K. P. and R. P. Singh, *Supercond. Sci. Technol.* **34**, 055003 (2021).
- [25] Arushi, D. Singh, A. D. Hillier, M. S. Scheurer, and R. P. Singh, *Phys. Rev. B* **103**, 174502 (2021).
- [26] K. Górnicka, X. Gui, B. Wiendlocha, L. T. Nguyen, W. Xie, R. J. Cava, and T. Klimczuk, *Adv. Funct. Mater.* **31**, 2007960 (2021).
- [27] Y. Gao, J.-F. Zhang, S. A. Yang, K. Liu, and Z.-Y. Lu, *Phys. Rev. B* **103**, 125154 (2021).
- [28] J. E. Sonier, J. H. Brewer, and R. F. Kiefl, *Rev. Mod. Phys.* **72**, 769 (2000).
- [29] S. Blundell, R. De Renzi, T. Lancaster, and F. Pratt, *Introduction to Muon Spectroscopy* (Oxford University Press, Oxford, 2021).
- [30] A. D. Hillier, S. Blundell, I. McKenzie, I. Umegaki, L. Shu, J. A. Wright, T. Prokscha, F. Bert, K. Shimomura, A. Berlie, H. Alberto, and I. Watanabe, *Nat. Rev. Methods Primers* **2**, 4 (2022).
- [31] A. Amato, H. Luetkens, K. Sedlak, A. Stoykov, R. Scheuermann, M. Elender, A. Raselli, and D. Graf, *Rev. Sci. Instrum.* **88**, 093301 (2017).
- [32] A. Suter and B. Wojek, *Phys. Procedia* **30**, 69 (2012).
- [33] N. R. Werthamer, E. Helfand, and P. C. Hohenberg, *Phys. Rev.* **147**, 295 (1966).
- [34] M. Tinkham, *Introduction to Superconductivity* (Krieger, Malabar, FL, 1975).
- [35] R. Kubo and T. Toyabe, in *Magnetic Resonance and Relaxation*, edited by R. Blinc (North-Holland, Amsterdam, 1967), p. 810; T. Toyabe, M. S. thesis, University of Tokyo, 1966.
- [36] G. M. Luke, Y. Fudamoto, K. M. Kojima, M. I. Larkin, J. Merrin, B. Nachumi, Y. J. Uemura, Y. Maeno, Z. Q. Mao, Y. Mori, H. Nakamura, and M. Sgrist, *Nature (London)* **394**, 558 (1998).
- [37] E. H. Brandt, *Phys. Rev. B* **37**, 2349 (1988).
- [38] E. H. Brandt, *Phys. Rev. B* **68**, 054506 (2003).
- [39] R. Prozorov and R. W. Giannetta, *Supercond. Sci. Technol.* **19**, R41 (2006).
- [40] A. Carrington and F. Manzano, *Physica C* **385**, 205 (2003).
- [41] Y. Nakajima, H. Hidaka, T. Nakagawa, T. Tamegai, T. Nishizaki, T. Sasaki, and N. Kobayashi, *Phys. Rev. B* **85**, 174524 (2012).
- [42] J. Hänisch, K. Iida, F. Kurth, E. Reich, C. Tarantini, J. Jaroszynski, T. Förster, G. Fuchs, R. Hühne, V. Grinenko, L. Schultz, and B. Holzapfel, *Sci. Rep.* **5**, 17363 (2015).
- [43] V. G. Kogan and R. Prozorov, *Phys. Rev. B* **90**, 100507(R) (2014).
- [44] Z. Guguchia, F. von Rohr, Z. Shermadini, A. T. Lee, S. Banerjee, A. R. Wieteska, C. A. Marianetti, B. A. Frandsen, H. Luetkens, Z. Gong, S. C. Cheung, C. Baines, A. Shengelaya, G. Taniashvili, A. N. Pasupathy, E. Morenzoni, S. J. L. Billinge, A. Amato, R. J. Cava, R. Khasanov *et al.*, *Nat. Commun.* **8**, 1082 (2017).
- [45] Y. J. Uemura, L. P. Le, G. M. Luke, B. J. Sternlieb, W. D. Wu, J. H. Brewer, T. M. Riseman, C. L. Seaman, M. B. Maple, M. Ishikawa, D. G. Hinks, J. D. Jorgensen, G. Saito, and H. Yamochi, *Phys. Rev. Lett.* **66**, 2665 (1991).
- [46] Y. J. Uemura, G. M. Luke, B. J. Sternlieb, J. H. Brewer, J. F. Carolan, W. N. Hardy, R. Kadono, J. R. Kempton, R. F. Kiefl, S. R. Kreitzman, P. Mulhern, T. M. Riseman, D. L. Williams, B. X. Yang, S. Uchida, H. Takagi, J. Gopalakrishnan, A. W. Sleight, M. A. Subramanian, C. L. Chien, M. Z. Cieplak *et al.* *Phys. Rev. Lett.* **62**, 2317 (1989).
- [47] Y. J. Uemura, A. Keren, L. P. Le, G. M. Luke, B. J. Sternlieb, W. D. Wu, J. H. Brewer, R. L. Whetten, S. M. Huang, Sophia Lin, R. B. Kaner, F. Diederich, S. Donovan, G. Grüner, and K. Holczer, *Nature (London)* **352**, 605 (1991).
- [48] G. Prando, Th. Hartmann, W. Schottenhamel, Z. Guguchia, S. Sanna, F. Ahn, I. Nekrasov, C. G. F. Blum, A. U. B. Wolter, S. Wurmehl, R. Khasanov, I. Eremin, and B. Büchner, *Phys. Rev. Lett.* **114**, 247004 (2015).
- [49] Z. Guguchia, A. Amato, J. Kang, H. Luetkens, P. K. Biswas, G. Prando, F. von Rohr, Z. Bukowski, A. Shengelaya, H. Keller, E. Morenzoni, Rafael M. Fernandes, and R. Khasanov, *Nat. Commun.* **6**, 8863 (2015).
- [50] D. Das, R. Gupta, C. Baines, H. Luetkens, D. Kaczorowski, Z. Guguchia, and R. Khasanov, *Phys. Rev. Lett.* **127**, 217002 (2021).
- [51] A. Shengelaya, R. Khasanov, D. G. Eshchenko, D. Di Castro, I. M. Savić, M. S. Park, K. H. Kim, Sung-Ik Lee, K. A. Müller, and H. Keller, *Phys. Rev. Lett.* **94**, 127001 (2005).
- [52] D. Das, K. Kobayashi, M. P. Smylie, C. Mielke, III, T. Takahashi, K. Willa, J.-X. Yin, U. Welp, M. Z. Hasan, A. Amato, H. Luetkens, and Z. Guguchia, *Phys. Rev. B* **102**, 134514 (2020).
- [53] D. T. Adroja, A. Bhattacharyya, M. Telling, Yu. Feng, M. Smidman, B. Pan, J. Zhao, A. D. Hillier, F. L. Pratt, and A. M. Strydom, *Phys. Rev. B* **92**, 134505 (2015).